

# FERRUM: A New Highly Efficient Spin Detector for Electron Spectroscopy\*

Matthias Escher, Nils B. Weber, and Michael Merkel<sup>†</sup>  
 FOCUS GmbH, Neukirchner Str.2, Hünstetten, D-65510, Germany

Lukasz Plucinski and Claus M. Schneider  
 Peter Grünberg Institut PGI-6, Forschungszentrum Jülich GmbH, Jülich, D-52428, Germany  
 (Received 30 June 2011; Accepted 17 August 2011; Published 17 September 2011)

To overcome the restrictions of conventional spin detectors (Mott, SPLEED) low energy electron scattering at a Fe(100)-p(1×1)O surface was first proposed by Bertacco and Ciccacci [Phys. Rev. B **59**, 4207 (1999)] as a system for highly efficient spin detection. We developed a new instrument based on that scheme. The iron is prepared *in-situ* on a W(100) crystal without the need for separate sample preparation and exchange when using a MgO substrate. Our working point at 6.5 eV scattering energy is consistent with the above paper by Bertacco and Ciccacci. Results obtained with UPS on an Fe film are shown. With a Sherman-function of approx. 30% and a reflectivity of up to 10% the figure of merit (FOM) is more than one magnitude higher compared to conventional detectors. The FOM shows no degradation over days in UHV. [DOI: 10.1380/ejsnt.2011.340]

Keywords: Spin detection; Electron spectroscopy

## I. INTRODUCTION

A major challenge in modern high-resolution electron spectroscopy lies in an efficient quantification of the electron spin polarization. A spin detection mechanism based on the exchange scattering of electrons at a magnetized target has already been shown in 1989 [1] to be a viable alternative to detectors based on spin-orbit scattering. A spin detector based on this effect has been described by Hillebrecht *et al.* [2]. Depending on the relative orientation of the electron-spins and the target magnetization the reflected electron intensity shows a high asymmetry at low kinetic electron energies. However, ferromagnetic scattering targets must be prepared as thin films and are quite sensitive to surface contamination by adsorbates. A breakthrough has been achieved recently by Bertacco *et al.* [3, 4] by passivating an iron film with oxygen. This is the spin-polarization principle used in the new detector, called FERRUM, the name indicating that an iron (lat. ferrum) film is the basis of the detector.

The oxidized iron film is easily prepared *in-situ* on a W(100) single crystal as substrate. First the W(100) crystal is cleaned then the iron is deposited with high purity by e-beam evaporation. After oxygen dosing, the iron film is insensitive to contaminations from residual gases, enabling one to work over weeks without preparation of a new iron film. Details about the underlying principle of the polarization-detection can be found in Ref. [3], examples of detectors based on the same principle can also be found in the literature [4–6].

## II. LAYOUT OF THE INSTRUMENT

A schematic representation of the FERRUM layout is shown in Fig. 1 whereas Fig. 2 shows a photograph of the

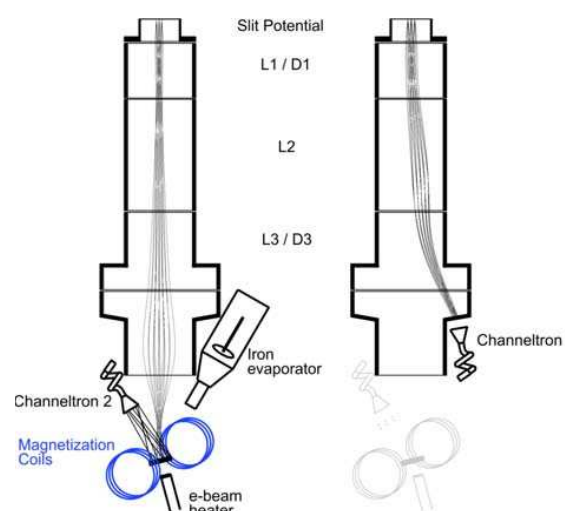


FIG. 1: Operational scheme of the FERRUM spin-detector: left: spin-resolved measurement mode. An iron film is evaporated onto the scattering target and magnetized by one of two orthogonal pairs of coils. Electrons are focused from the analyzer exit slit onto the scattering target and counted by the channeltron 2. right: integral intensity measurement. The electron beam is deflected and focused into the off-axis channeltron 1 by two deflectors integrated into the transfer lens.

detector. The heart of the detector consists of an iron film deposited onto a W(100) single crystal used as substrate. In advance of the iron deposition the tungsten crystal is prepared by heating in oxygen to approx. 1200 K to remove carbon contaminants and high temperature flashes (2200 K) to remove oxides [7]. This preparation can be done *in-situ* without the need for target transfer or a separate preparation chamber as it is the case when using MgO as substrate [4, 6]. For the iron deposition we use a modified FOCUS EFM 3 e-beam evaporator. It is integrated into the whole assembly pointing towards the tungsten crystal. The oxygen is provided by a heated silver tube from atmosphere. The heated silver selectively allows oxygen to diffuse from atmosphere into the vacuum. An oxygen partial pressure of typical  $5 \times 10^{-8}$  mbar

\*This paper was presented at 8th International Symposium on Atomic Level Characterizations for New Materials and Devices, Olympic Parktel, Seoul, Republic of Korea, 22-27 May, 2011.

<sup>†</sup>Corresponding author: m.merkel@focus-gmbh.com



FIG. 2: Photograph of the FERRUM spin-detector. The detector is mounted on a CF100 flange. Chamber and  $\mu$ -metal screens are removed for clarity.

for 10 min is used to passivate the iron film.

For preparation of a new iron film a single high temperature flash of the tungsten crystal is sufficient to clean it up for a new preparation cycle.

Two channel electron multipliers (channeltrons 1 and 2) are used to collect both the unfiltered integral and the spin-resolved count-rates.

To measure the integral intensity the incoming electron beam is accelerated and deflected electrostatically into the first channeltron. For the spin resolved counting channel the beam remains undeflected. The electrons leaving the analyzer exit slit are then focused by a dedicated zoom-lens system onto the iron film. The lens system operates for a large range of retardations so that either different analyzer pass energies and/or different scattering energies can be used without loss of transmission. After scattering at the iron film electrons are collected with the second channeltron positioned at a  $15^\circ$  off normal in backwards direction.

To select the detector spin orientation two pairs of coils are used to switch the magnetization of the iron film in both in-plane directions to access the two orthogonal spin components. The magnetization coils are driven by a dedicated magnetic pulse control unit what is fully computer controlled.

By this way no mechanical movement is needed to switch between the spin and the integral channel and between the two orthogonal spin-orientations in the spin filtered channel. This ensures a high reproducibility of the results and enables an easy and automated operation also.

To enable optimum operation at very low energies the detector is housed completely in a double mu-metal shielded UHV chamber. The whole assembly is build up on a DN100CF base flange.

For the purpose of our current study the FERRUM detector has been combined with the cylindrical sector analyzer FOCUS CSA 300. Generally the detector can be combined with other energy filters also. The prototype detector is prepared to be used with a high-end hemispherical analyzer (MBS-A1 of MB Scientific). In this case an additional  $90^\circ$  deflector between exit slit and FERRUM detector will be used to get access to both the in-plane and out-of-plane components of the electron spin polarization at the sample.

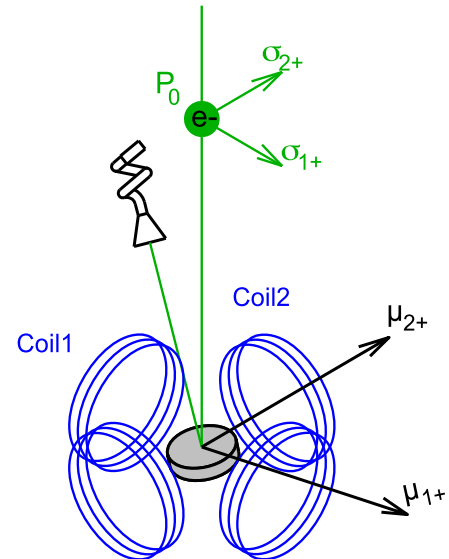


FIG. 3: Scheme of the scattering geometry. Electrons having a spin-polarization  $\sigma$  are scattered by the magnetized iron film with magnetization  $\mu$ . The magnetization can be switched in four different states by two pairs of coils. The scattering plane is defined by the incoming and scattered beams. A scattering target magnetization  $\mu_1$  in this plane is generated by the first pair of coils (coil 1). For spin-polarizations perpendicular to the scattering plane (direction along coil 2), also spin-orbit asymmetries can be present.

### III. CHARACTERIZATION OF THE SPIN DETECTOR

We have characterized the properties of the spin detector using secondary electrons ( $E_{\text{kin}} \approx 1$  eV) excited by VUV-light ( $h\nu = 21.2$  eV) from a magnetized iron film deposited on W(110). The secondary electrons spin polarization is estimated to be  $P_0 = 0.3$  [8] and can be switched along the easy axis of the iron film. A sketch of the scattering geometry is shown in Fig. 3, where direction 2 coincides with the easy axis of the iron film and thus the spin-polarization direction. The scattered intensity can be measured both as a function of the spin-polarization of the electrons and the magnetization of the detector iron film. In the description of the experiment we follow the definitions and formula outlined by Bertacco and Ciccacci [3]. The measured intensity  $I$  of the reflected electrons depends on the magnitude  $P_0$  of the electron spin-polarization and its direction  $\sigma$ , the magnetization direction  $\mu$  of the detector crystal, the exchange coupling constant  $A_{\text{ex}}$  and the spin-orbit coupling constant  $A_{\text{so}}$  as:

$$I_{\mu}^{\sigma} = \alpha I_0 (1 + \mu \sigma P_0 A_{\text{ex}} + \sigma P_0 A_{\text{so}}), \quad (1)$$

where  $\alpha$  is the spin-independent reflectivity of the scattering target and  $I_0$  the primary intensity. Four measurements with different combinations of the spin- and magnetization directions can be performed and give the intensities  $I_{+}^{+}$ ,  $I_{-}^{+}$ ,  $I_{+}^{-}$  and  $I_{-}^{-}$ . Two asymmetries for constant magnetization direction  $\mu$  are defined as

$$A_{+} = \frac{I_{+}^{+} - I_{+}^{-}}{I_{+}^{+} + I_{+}^{-}}, \quad A_{-} = \frac{I_{-}^{+} - I_{-}^{-}}{I_{-}^{+} + I_{-}^{-}}. \quad (2)$$

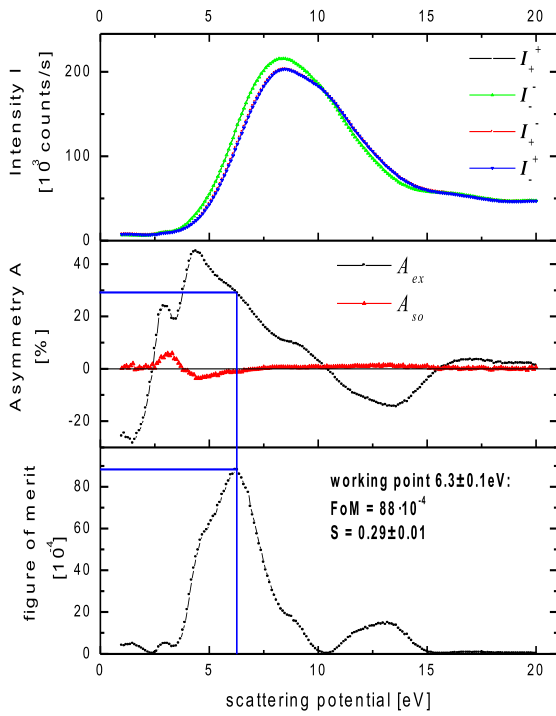


FIG. 4: Characterization measurement of the spin-detector. Top: scattered electron intensity as a function of the scattering potential for four different combinations of electron spin polarization  $\sigma$  and scattering target magnetization  $\mu$  direction both lying in plane 2 as defined in Fig. 3. The electron spin polarization was  $P_0 = 0.3$ . Middle: Exchange and spin-orbit asymmetry term calculated with (2) and (3) from the raw data in the top panel. Bottom: Figure of merit  $A^2 \cdot I/I_0$  as a function of the scattering potential. At the working point of 6.3 eV a reflectivity  $I/I_0$  of 10.6% has been measured.

These asymmetries can be rewritten to give the coupling constants for exchange and spin-orbit interaction:

$$A_{so} = \frac{A_+ + A_-}{2P_0}, \quad A_{ex} = \frac{A_+ - A_-}{2P_0}. \quad (3)$$

Figure 4 shows a characterization measurement. In the top panel the raw intensities are plotted. Pairs of measurements with both parameters  $\sigma$  and  $\mu$  switched, i.e.  $I_+^+$ ,  $I_-^+$  or  $I_-^-$  and  $I_+^-$ , nearly match except in that region where a substantial spin-orbit-coupling is observed.

The exchange and spin-orbit asymmetries extracted from these measurements using Eqs. (2) and (3) are plotted in the middle panel of Fig. 4. The exchange asymmetry has two pronounced maxima with different signs at about 4.5 eV and 3.2 eV. The spin-orbit asymmetry is much smaller and can be neglected outside the range between about 2 eV and 6 eV. At the detectors working point of  $6.3 \pm 0.1$  V the spin-orbit asymmetry is smaller than 1%.

To fix the working point of the detector, a figure of merit  $FoM = I/I_0 \cdot A^2$  has been evaluated and is shown in the bottom panel of Fig. 4. It reaches its maximum of about  $8.8 \times 10^{-3}$  at a scattering potential of  $6.3 \pm 0.1$  eV, where a reflectivity of approx. 10.6% has been measured. Taking into account that two consecutive measurements with opposite  $\mu$  have to be done to get one polarization



FIG. 5: Photograph of the FERRUM spin detector mounted (at the left hand site) at the exit flange of a cylinder sector analyzer CSA 300. The analyzer entrance lens (right) is covered by a protection cylinder. The analyzer mu-metal chamber is directly connected to the detector double mu-metal shielded chamber. The Fe-deposition source and the thermal oxygen doser are integrated with the detector housing. Because of the 90 deflection of this analyzer no additional deflector is needed to measure in- and out-of-plane spin components.

direction the calculated figure of merit has to be halved to  $4.4 \times 10^{-3}$  for one spin component and to  $2.2 \times 10^{-3}$  for both orthogonal spin components.

To extract an unknown electron spin polarization  $P_0$ , at least two measurements for each spin-component have to be done. In this case the unknown spin-polarization of the electrons  $\sigma$  is not changed and the magnetization of the scattering target is switched. The spin polarization  $P$  of the electron beam

$$P = \frac{1}{S} \cdot \frac{I_+^\sigma - I_-^\sigma}{I_+^\sigma + I_-^\sigma}, \quad (4)$$

can be calculated, where  $S$  is the so called Sherman function of the detector. Substituting Eq. (1) into Eq. (4) it can be shown that the Sherman function  $S$  equals the exchange asymmetry  $A_{ex}$  if the spin-orbit coupling constant  $A_{so}$  can be neglected. In the maximum of the figure of merit (see Fig. 4, bottom), representing the working point of the detector, the spin-orbit coupling term becomes negligible compared to the  $A_{ex}$ , therefore the Sherman function for this energy can directly be read from the asymmetry curve in Fig. 4. We derived for the Sherman function  $S = 0.29 \pm 0.01$  at the working point of about  $6.3 \pm 0.1$  eV scattering potential, assuming a secondary electron spin polarization  $P$  of 30% [8]. As the measured asymmetry depends on the exchange scattering term only, the spin detection is independent of the orientation of spin and magnetization with respect to the scattering plane.

A practical way to minimize the influence of the intensity drift affecting the asymmetry measurement is a time-symmetric sequence of measurements with opposite scattering target magnetization as described in Ref. [5]. In our case this procedure proved sufficient to prevent false asymmetries due to drift in the excitation intensity. After preparation of the scattering target we used the detector for several weeks. During this time we did not observe any significant change in asymmetry and/or reflectivity. The oxygen passivation of the iron target delivers a very stable and rigid behavior of the detector.

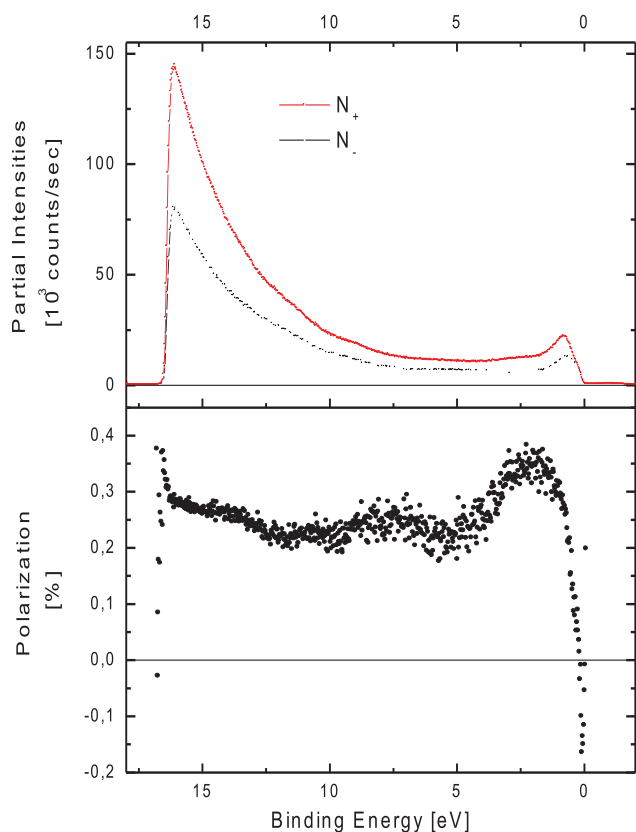


FIG. 6: UPS-spectrum of Fe on W(110) Measured with the CSA 300 cylinder sector analyzer as shown in Fig. 5 (approx. 50 meV energy resolution) and using a VUV gas discharge lamp ( $h\nu = 21.2$  eV) for excitation.

#### IV. TEST MEASUREMENTS AT FE ON W(110)

We have used the system Fe on W(110) as our exemplary reference for spin-resolved valence band spectra. The iron film has been prepared in situ with e-beam evaporation. The FERRUM detector mounted to the CSA300 is shown in Fig. 5. The energy resolution of the experiment was approximately 50 meV ( $E_{\text{pass}} = 4$  eV, entrance and exit slit 3 mm). As excitation source we have used a FOCUS HIS13 VUV-discharge lamp operated with He I

light ( $h\nu = 21.2$  eV). One spin-component was measured using two energy scans with reversed scattering target magnetization ( $\mu = \pm 1$ ). The resulting spin resolved valence band spectra and the measured spin polarization are shown in Fig. 6.

#### V. SUMMARY

We described a newly developed spin detector which is based on the exchange scattering of electrons on a magnetized and oxygen-passivated iron film. The spin detector has been tested and well characterized in combination with a standard energy analyzer. Our results agree very well with the proof of principle experiments published by Bertacco *et al.* [4].

We see two major design advantages of the detector. First there is no need of transfer of the scattering target or separate substrate preparation facilities since the W crystal used as substrate for the iron film is easy to prepare on site of the detector. Second any further mechanical manipulation of the scattering target for choosing the spin direction is unnecessary as the two pairs of magnetization coils switch the spin direction to be analyzed. In that way an automated and highly reproducible operation of the detector is possible. Furthermore a compact footprint and flexible transfer optics guarantees for an easy integration of the detector into existing experimental setups and the possibility to adapt it to different electron energy analyzers.

These features enable the FERRUM detector to fully exploit the physical advantages of its underlying principle: The large figure of merit, being at least one magnitude higher than existing Mott [9, 10] or SPLEED [11] detectors and the long lifetime of the scattering target that remains nearly unchanged over several weeks without the need of a new film preparation.

We expect for the near future that a number of spin resolved experiments will take advantage of this instrumental approach that is now available. In particular the energy resolution of spin-resolved photoemission experiments can be improved and/or their acquisition time can be reduced essentially.

- 
- [1] D. Tillmann, R. Thiel, and E. Kisker, *Z. Physik B* **77**, 1 (1989).
- [2] F. U. Hillebrecht, R. M. Jungblut, L. Wiebusch, Ch. Roth, H. B. Rose, D. Knabben, C. Bethke, N. B. Weber, St. Manderla, U. Rosowski, and E. Kisker, *Rev. Sci. Instrum.* **73**, 1229 (2002).
- [3] R. Bertacco and F. Ciccacci, *Phys. Rev. B* **59**, 4207 (1999).
- [4] R. Bertacco, D. Onofrio, and F. Ciccacci, *Rev. Sci. Instrum.* **70**, 3572 (1999).
- [5] A. Winkelmann, D. Hartung, H. Engelhard, C.-T. Chiang, and J. Kirschner, *Rev. Sci. Instrum.* **79**, 083303 (2008).
- [6] T. Okuda, Y. Takeichi, Y. Maeda, A. Harasawa, I. Matsuda, T. Kinoshita, and A. Kakizaki, *Rev. Sci. Instrum.* **79**, 123117 (2008).
- [7] Kh. Zakeri, T. R. F. Peixoto, Y. Zhang, J. Prokop, and J. Kirschner, *Surf. Sci.* **604**, L1 (2010).
- [8] J. Kirschner and K. Koike, *J. Phys. D: Appl. Phys* **25**, 1139 (1992).
- [9] L. G. Gray, W. M. Hart, F. B. Dunning, and G. K. Walters, *Rev. Sci. Instrum.* **55**, 88 (1984).
- [10] G. C. Burnett, T. J. Munroe, and F. B. Dunning, *Rev. Sci. Instrum.* **65**, 1893 (1994).
- [11] D. Yu, Ch. Math, M. Meier, M. Escher, G. Rangelov, and M. Donath, *Surf. Sci.* **601**, 5803 (2007).